Bioresource Technology 359 (2022) 127400

Contents lists available at ScienceDirect

Bioresource Technology

journal homepage: www.elsevier.com/locate/biortech

Anaerobic digester microbiome dynamics in response to moderate and failure-inducing shock loads of fats, oils and greases

Ashley E. Berninghaus, Tyler S. Radniecki *

School of Chemical, Biological, and Environmental Engineering, Oregon State University, Corvallis, OR 97331 USA

HIGHLIGHTS

- Sequential moderate shocks result in a resilient and specialized community.
- Sub-dominant bacterial populations are largely responsible for stable operation.
- There are distinct early and late recovery communities post-failure.
- Post-failure recovery results in an entirely new unadapted community structure.
- Small and moderate FOG shock loads lead to adaptation, failure events do not.

GRAPHICAL ABSTRACT

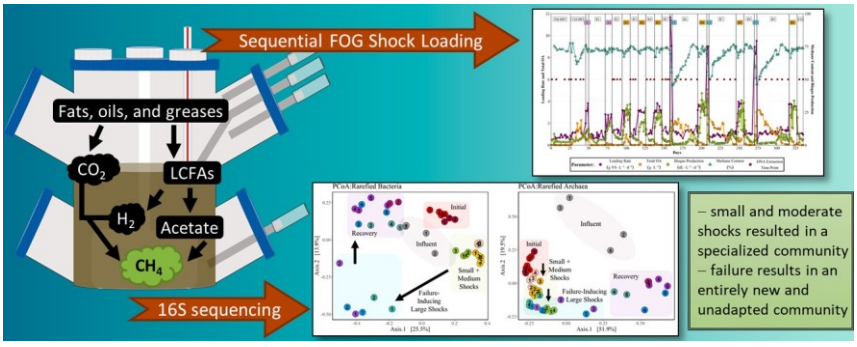

ARTICLE INFO

Keywords:
Co-digestion
Sub-dominant bacteria
Perturbation
Methanogens
Acclimation

ABSTRACT

Accidental organic overloading (shock loading) is common during the anaerobic co-digestion of fats, oils and greases (FOG) and may lead to decreased performance or reactor failure due to the effects on the microbiome. Here, adapted and non-adapted lab-scale anaerobic digesters were exposed to FOG shocks of varying organic strengths. The microbiome was sequenced during the recovery periods employed between each shock event. Non-failure-inducing shocks resulted in enrichment of fermentative bacteria, and acetoclastic and methylotrophic methanogens. However, sub-dominant bacterial populations were largely responsible for increased biogas production observed after adaptation. Following failure events, early recovery communities were dominated by *Pseudomonas* and *Methanosaeta* while late recovery communities shifted toward sub-dominant bacterial taxa and *Methanosarcina*. Generally, the recovered microbiome structure diverged from that of both the initial and optimized microbiomes. Thus, while non-failure-inducing FOG shocks can be beneficial, the adaptations gained are lost after a failure event and adaptation must begin again.

Abbreviations: AD, anaerobic digestion; FOG, fats, oils, and greases; VS, volatile solids; OA, organic acid; OLR, organic loading rate; LCFA, long-chain fatty acid; rRNA, ribosomal ribonucleic acid; PCoA, principal coordinates analysis; RAS, recycled activated sludge; DNA, deoxyribonucleic acid; PCR, polymerase chain reaction; ASV, amplicon sequence variant; COD, chemical oxygen demand; TWAS, thickened waste activated sludge.

* Corresponding author at: 105 SW 26th St, Corvallis, OR 97331.
E-mail address: tyler.radniecki@oregonstate.edu (T.S. Radniecki).

https://doi.org/10.1016/j.biortech.2022.127400
Received 28 February 2022; Received in revised form 26 May 2022; Accepted 28 May 2022
Available online 30 May 2022

1. Introduction

The natural production of methane via anaerobic digestion (AD) is facilitated by a complex community of microorganisms, primarily bacteria and archaea, referred to as the AD microbiome. AD is growing in prominence as a solution to the disposal of food waste, sewage sludge, and the organic fraction of municipal solid waste while simultaneously increasing methane production. Specifically, the anaerobic co-digestion of energy-rich fats, oils, and greases (FOG) has been recognized as an effective and commercially viable approach to increase energy recovery at wastewater treatment facilities (Li et al., 2013). Despite the reported benefits of co-digestion, intensification of the FOG co-digestion process and efforts to predict reactor response to process changes have been hampered by a limited fundamental understanding of how the AD microbiome responds to process disturbances (Salama et al., 2019).

Microbial shifts have been observed with the introduction of FOG as a co-substrate. Specifically, within the bacterial domain, the enrichment of fermentative bacteria from the *Synergistetes*, *Actinobacteria*, *Firmicutes*, *Bacteroidetes*, *Chloroflexi* and *Proteobacteria* phyla have been observed (Amha et al., 2017; Ferguson et al., 2018; Kurade et al., 2019; Wang et al., 2018; Yang et al., 2016). Within the archaeal domain, acetoclastic methanogenesis by *Methanosaeta*, an obligate acetate user, is typically considered the dominant methanogenic pathway (Kurade et al., 2019). However, *Methanosaeta* are sensitive to the increases in organic loading rates, salt, and ammonia−nitrogen concentrations that result from the introduction of FOG (Kurade et al., 2019). This results in a shift of the acetoclastic pathway towards *Methanosarcina,* a metabolically and physiologically diverse methanogenic genera, and towards an increased abundance of obligate hydrogenotrophic methanogens from the orders *Methanobacteriales* and *Methanomicrobiales* (Amha et al., 2017; De Vrieze et al., 2012).

While the adaption of AD microbiomes to non-inhibitory concentrations of FOG (Silvestre et al., 2011) and long-chain fatty acids (LCFAs) have been characterized previously (Kougias et al., 2016), there is still a limited understanding of how AD microbiomes respond to failure-inducing conditions. Studies that have examined the recovery of AD microbiomes after process failure utilized organic loading rates (OLRs) that were increased gradually over long periods of time (ranging between 20 and 80 days in length), to induce process failure (Wang et al., 2020). However, in the field, AD failure is commonly due to a relatively discrete, short-term accidental overfeeding event, known as a shock load. To the author's knowledge, no studies have investigated short, intense shock loads and their subsequent effect on the AD microbiome.

To address this knowledge gap, the interaction between FOG shock loads and the response of the AD microbiome was investigated. This was achieved by: (i) comparing the differences in responses between AD microbiomes adapted to FOG and those that were not and (ii) characterizing the AD microbiome response to non-failure and failure-inducing shock loads. The physical data associated with the operation of these experiments have been previously described (Berninghaus and Radniecki, 2022). In the present study, archaeal and bacterial community dynamics were monitored using high-throughput Illumina MiSeq 16S rRNA amplicon sequencing. Bioinformatics tools (principal coordinate analysis (PCoA), alpha diversity (Shannon's Index), Raup and Crick dissimilarity index, and Pearson correlations) were used to gain insight into the microbiome's response to the various intensities of the shock loads.

2. Materials and methods

2.1. Experimental set up and operation

2.1.1. Source of seed anaerobic digestate and fats, oils, and greases

Seed anaerobic digestate and recycled activated sludge (RAS) were collected from a full-scale mesophilic anaerobic digester at the City of Corvallis Wastewater Reclamation Plant (Corvallis, OR) and FOG was collected from the FOG receiving station at the City of Gresham Wastewater Reclamation Plant (Gresham, OR), as previously described (Berninghaus and Radniecki, 2022).

2.1.2. Long-term shock study

The long-term shock study was run for 335 days divided into 11 shock (A1-2, B1-6, and C1-3) and 10 recovery (R1-10) phases. Full details on the operation of this study have been previously described (Berninghaus and Radniecki, 2022). In brief, the reactor experienced two different modes of operation: shock periods, defined as periods of high OLRs where a mixture of RAS and FOG was fed, and recovery periods, defined as periods of low OLRs where only RAS was fed. Shock A, the lowest organic load (2.53 ± 0.49 g VS/L·d), was administered twice with a mixture of RAS and FOG, 1:1 (v/v %). Shock B, the second largest organic load (3.27 ± 0.11 g VS/L·d), was administered six times with a mixture of RAS and FOG 3:7 (v/v). Shock C, the largest organic load (9.36 ± 0.75 g VS/L·d), was administered three times with a mixture of RAS and thickened FOG, 2:8 (v/v). Following each shock period, the reactor went into recovery until organic acid levels were below 50 mg/L and biogas production stabilized.

2.1.3. Single shock studies

Both single shock studies were run side-by-side for a total of 100 days to study the response of a non-adapted reactor to an organic overload event, as previously described (Berninghaus and Radniecki, 2022). Reactor 1 received a single C shock (1:4 (v/v) RAS:FOG), while Reactor 2 received a single B shock (3:7 (v/v) RAS:FOG). Following these single shock events, both reactors were fed only RAS during the recovery phase.

2.2. Analytical methods

Biogas production, biogas composition, pH, conductivity, dissolved *ortho*-phosphate, dissolved total ammonia nitrogen, total solids, volatile solids, and organic acid concentrations were measured as previously described (Berninghaus and Radniecki, 2022).

2.3. DNA Extraction

DNA was extracted from 500 μL aliquots of homogenous anaerobic digestate sludge throughout each experiment (44 samples total for the long-term experiment and 12 samples total for each of the short-term experiments). DNA extractions were performed as previously described using the Qiagen DNeasy PowerSoil DNA Extraction Kit (Qiagen, Venlo, the Netherlands) according to manufacturer instructions (Berninghaus and Radniecki, 2021).

2.4. 16S rRNA gene sequences

The hypervariable V4 and V3 regions of the 16S gene were sequenced for both *Bacteria* and *Archaea* domains, respectively, via paired-end (2x300) sequencing on an Illumina MiSeq V3 platform following manufacturer instructions. For *Bacteria*, the V4 region was amplified with primers 515F and 806R (Apprill et al., 2015; Parada et al., 2016). For *Archaea*, the V3 region was amplified with primers Ar0787 and Ar1059 (Fischer et al., 2019; Yu et al., 2005). PCR and library preparation were conducted as previously described (Berninghaus and Radniecki, 2021).

2.5. Bioinformatics analysis

The obtained reads were processed using the DADA2 microbiome pipeline (available at https://github.com/benjjneb/dada2), as previously described (Berninghaus and Radniecki, 2021). The raw Illumina sequence data obtained were submitted to the National Centre for

Biotechnology Information's (NCBI) sequence read archive (SRA) data base. The following Bioproject numbers house this data: PRJNA803944 for the single moderate shock data, PRJNA804324 for the single large shock data, and PRJNA804334 for the long-term experiment data.

Sequences with<1,000 reads were removed from the datasets to reduce the number of spurious ASVs. Remaining sequences were rarefied to even depths to correct for sampling differences (Knight et al., 2018). Species richness (observed ASV counts) and evenness (Shannon's index) were calculated using R phyloseq (McMurdie and Holmes, 2013). Compositional differences between microbiomes were assessed using principle coordinate analysis (PCoA) using R phyloseq (McMurdie and Holmes, 2013) using the Bray-Curtis distance. Raup-Crick dissimilarities were calculated using R vegan (Chase et al., 2011; Jari Oksanen et al., 2020). Correlations with environmental data were performed using R microeco (Liu et al., 2020).

3. Results and discussion

3.1. Summary of physiological responses to FOG shock loading

A more detailed analysis of the physical and chemical parameters observed during these experiments has been previously reported (Berninghaus and Radniecki, 2022). In brief, the single B and C shock experiments experienced one single shock period after a start-up period (30 d HRT and 15 d HRT). Both of these single shock events resulted in reactor failure, indicated by a rapid decrease in biogas production, accumulation of organic acids (OAs), and a decrease in methane content (Fig. 1A and B). DNA was extracted in even time intervals throughout the initial phases and during the recovery period following each of the single shock events.

The long-term experiment was comprised of repeated shock events of varying organic loading rates (Fig. 1C). Shocks A1 and A2 exposed the reactor to FOG at lower FOG:RAS ratios before the moderate B-shocks were employed. During the first 3 successive B-shocks (B1-B3), gas production increased with the addition of FOG while methane content remained relatively stable. Additionally, OA accumulation decreased with each successive B-shock. The B-shocks were followed by failure-inducing C-shocks (C1-3), which resulted in rapid decreases in biogas productivity and methane content and large accumulations of OAs. DNA was extracted evenly during the initial phases and the recovery periods between the FOG shock loads.

3.2. General microbiome dynamics in response to FOG shock loads

Dynamic changes within the microbial community structure were observed throughout all experiments. During startup (100% TWAS, 0%

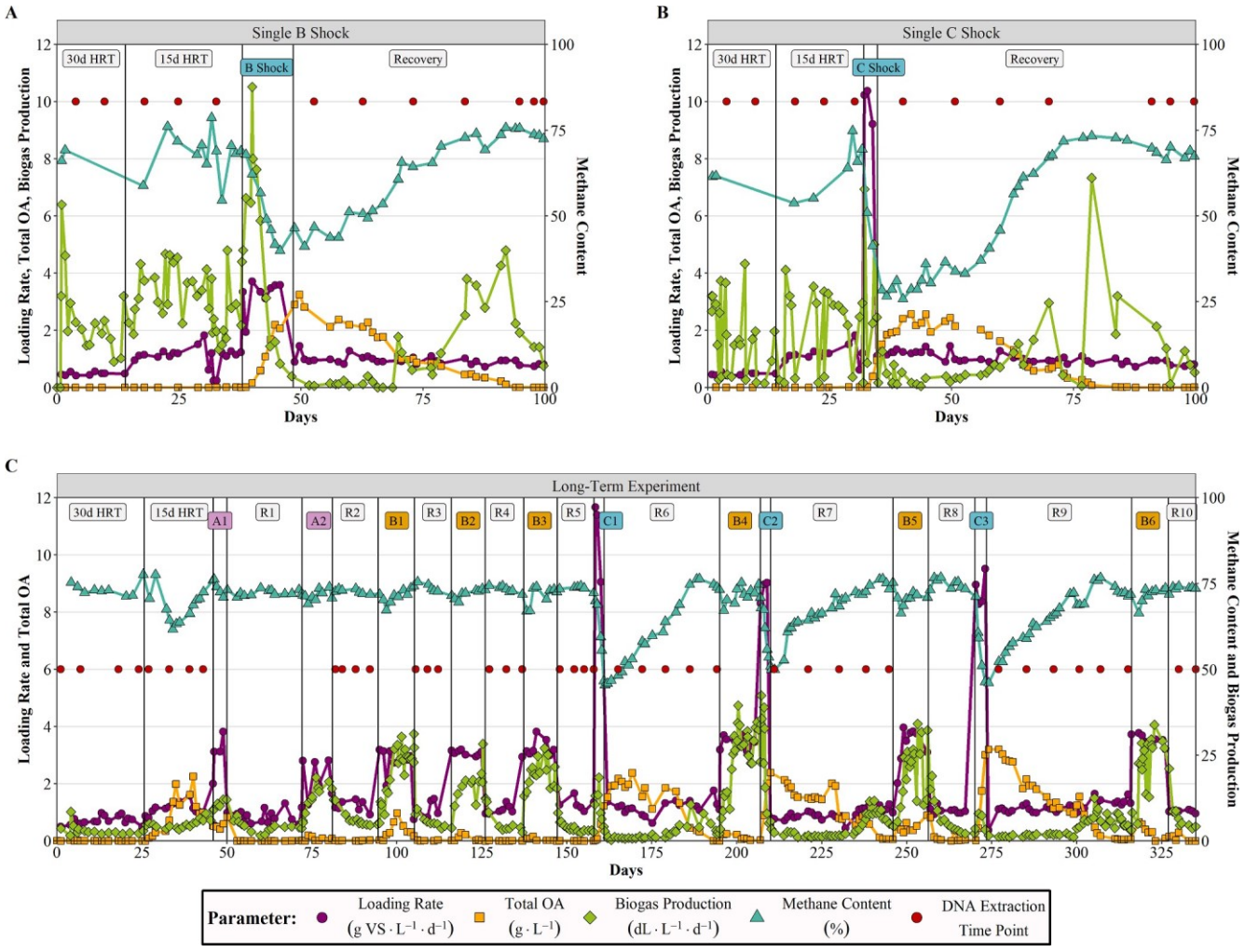

Fig. 1. Selected physical and chemical parameters from the single B shock (A), single C shock (B), and long-term (C) experiments. For the single shock experiments (A and B), organic loading rate, total organic acid (OA) content, and biogas production are shown on the left y-axis while methane content is shown on the right y-axis. For the long-term experiment (A), organic loading rate and total OA are shown on the left y-axis while biogas production and methane content are shown on the right y-axis. Black vertical lines designate the different phases of operation. Red circles denote time points where DNA was extracted. (For interpretation of the references to color in this figure legend, the reader is referred to the web version of this article.)

FOG), the bacterial and archaeal communities across all 3 experiments were similar with Raup and Crick dissimilarity index values of 0.001 for both bacteria and archaea. The Raup and Crick dissimilarity index ranges from 0, for identical communities, to 1, for communities with no similarity (based on ASV composition).

During the long-term experiment, exposure to a series of small shocks (A1-2) and moderate shocks (B1-3) resulted in a shift in the clustering of the AD microbiome from its initial configuration (Fig. 3). This new optimized configuration demonstrated enhanced biogas production rates and decreased levels of OA accumulation (Fig. 1C) (Berninghaus and Radniecki, 2022). Additionally, both the bacterial and archaeal communities demonstrated increased richness and Shannon's alpha diversity values (Fig. 2). The bacterial community saw richness increase by 10% (178.4 ± 10.0 to 196.9 ± 16.7) while the archaeal community increased by 28% (48.6 ± 5.6 to 62.4 ± 12.4) between the initial and optimized communities, respectively.

However, when the long-term reactor was subjected to disturbance-to-failure events, large C-shock loads, the microbial community structure became dissimilar from that of both of the initial and optimized clusters (Fig. 3). The dissimilarity index between the initial community configuration and shocks C1, C2, and C3 were 0.146, 0.999, and 0.954 for the bacterial domain and 0.368, 0.519, and 0.737 for the archaeal domain, respectively. In addition, these shifts corresponded with substantial decreases in richness and alpha diversity values (Fig. 2). The bacterial community richness values decreased, with decreases of 20%, 46%, and 39% observed for shocks C1, C2, and C3 compared to the optimized community. On the contrary, the archaeal community richness values actually increased by 4% for C1 and decreased by 16% and 19% for shocks C2 and C3, respectively, compared to the optimized community.

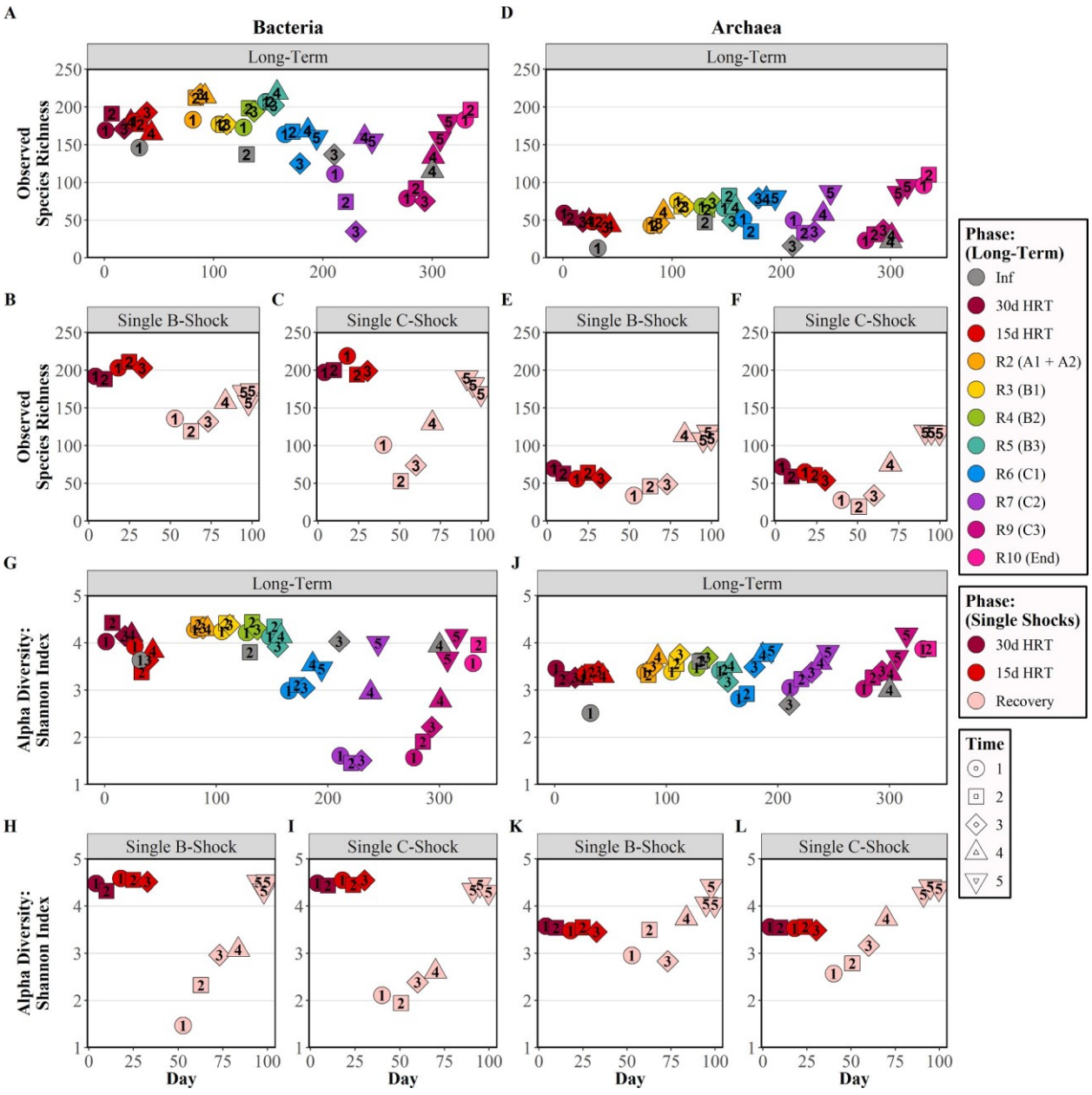

Fig. 2. Observed species richness for bacterial (A-C) and archaeal (D-F) domains separated by experiment. Shannon's Index alpha diversity values for the bacterial (G-I) and archaeal (J-L) domains. All samples are represented for each of the experiments shown. Each phase of interest has been given a unique color and is labeled with the relevant recovery period. The shock phase that preceded each recovery period is noted in parentheses. The time labels indicate sample order within each respective phase (i.e. 1 denotes the first time point within that phase).

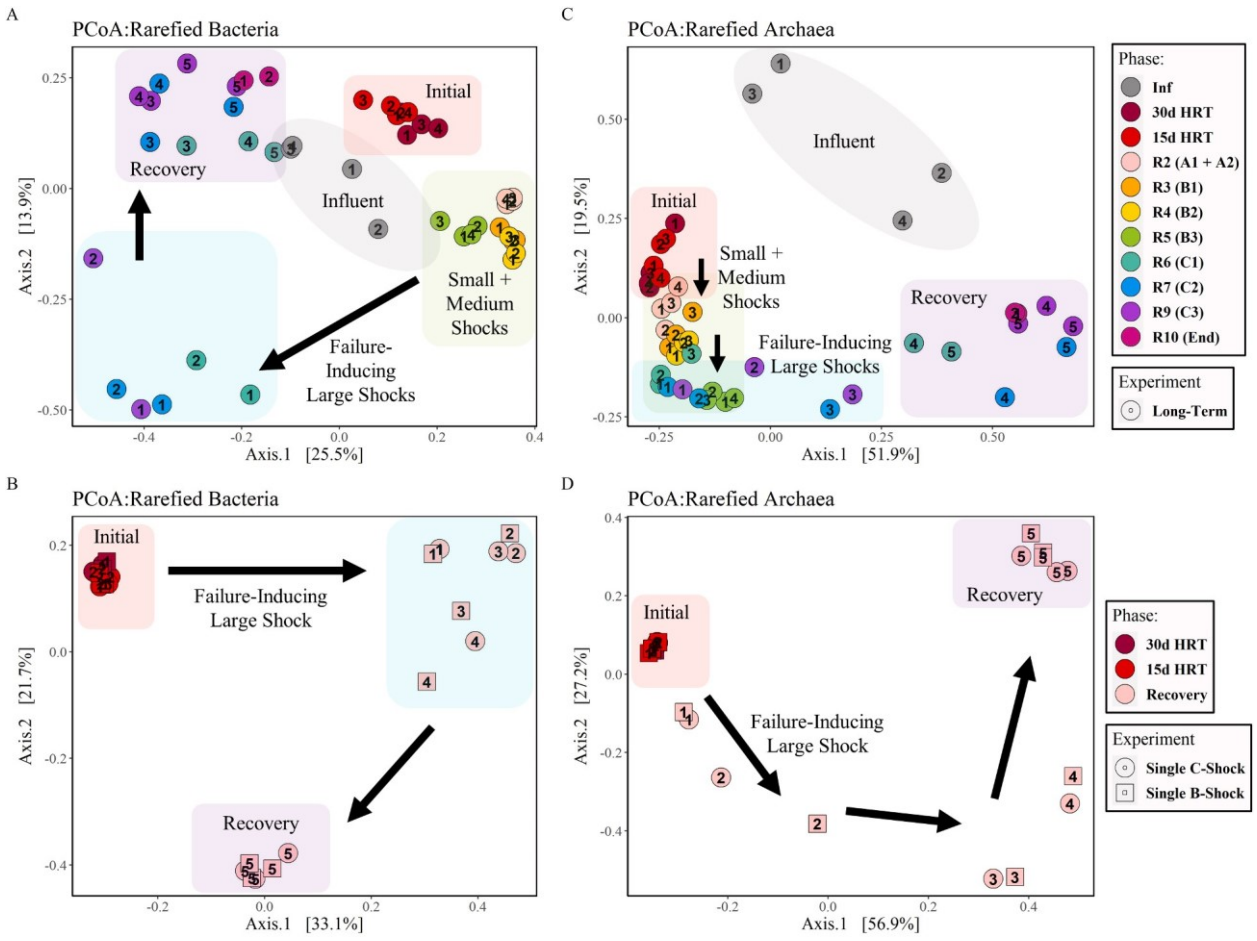

Fig. 3. Principle coordinate analysis (PCoA) based on Bray-Curtis distance for the bacterial and archaeal domains separated by experiment. All samples are represented for each of the experiments shown. The time labels indicate sample order within each respective phase. Shaded clusters are shown to highlight specific groups and are not statistically significant.

Similar trends were observed during the single-shock experiments. Both the single moderate B-shock and single large C-shock resulted in a disturbance-to-failure event which shifted the microbial community structure from its initial structure (Fig. 3C and D). Similar to the longterm experiment, these shifts corresponded with decreases in richness and alpha diversity values, with bacterial richness values again decreasing by a greater extent. The bacterial richness values decreased by 25% and 36% between the initial and recovery communities for the single B- and single C-shock loads, respectively (Fig. 2). Meanwhile, the archaeal community saw an increase of 17% and 33% for the same pairwise comparisons. In addition, the dissimilarity index values between the initial community and that of the post-failure community were 0.09 and 0.02 for the bacterial community while these same comparisons resulted in dissimilarity values of 1 for the archaeal community for both the single B- and single C-shock loads, respectively.

These decreases are likely due to the unique environment created within the reactor following a disturbance-to-failure event, including the build-up of OAs and changes in pH, nutrient content, and methane content (Berninghaus and Radniecki, 2022). This likely acted as a selective pressure resulting in fewer taxa present in both domains initially after shock loading events. For example, during the post-failure recovery periods, both the bacterial and archaeal domains exhibited "early recovery" and "late recovery" clusters in all experiments (Fig. 3). This mirrored changes in OA accumulation and degradation (Fig. 1C), suggesting that OAs are a strong selective pressure in the determination of the archaeal and bacterial community structure.

Interestingly, following recovery from a failure event, neither the bacterial nor the archaeal communities became similar to their pre-failure cluster, whether that be the initial or optimized microbiomes (Fig. 3). This was also reflected in the diversity metrics for the bacterial and archaeal domains but with opposite trends. For archaea, following recovery from a failure event, both the richness and Shannon alpha diversity values increased to levels greater than the initial and optimal communities. (Fig. 2 D-F and J-L). This observed increase in archaeal community diversity is likely due to the abundance and diversity of substrates available after FOG addition.

However, a different trend was observed in the bacterial domain. Following recovery from a failure event, both the bacterial richness and Shannon alpha-diversity values decreased to levels less than the initial and optimized communities (Fig. 2A-C and G-I). These decreases in richness and alpha-diversity had a negative effect on the long-term anaerobic digester microbiome's ability to tolerate and respond to future C-shock loads. For instance, immediately prior to the initial C-shock load (C1), the bacterial domain achieved its greatest richness values, and recovery from the failure-inducing event took 35 days for the depletion of accumulated OAs and 27.5 days for the recovery of methane production to pre-failure levels (Berninghaus and Radniecki, 2022).

However, prior to the C2 and C3 shock loads, the bacterial community was less rich than the optimized community, which resulted in longer recovery times of up to 43 days for OA degradation and up to 34.5 days to restore the methane content (Fig. 1). Additionally, with each successive C-shock, the recovered bacterial community became more dissimilar from the optimal community with dissimilarity indexes 0.01, 0.14, and 0.968 for the C1, C2, and C3 recovered communities,

respectively. Previous work has suggested that greater community diversity results in more robust function because of the functional redundancy provided (Wang et al., 2020; Werner et al., 2014).

Nonetheless, bacterial diversity alone does not predict performance. For instance, in the single shock experiments, the start-up communities had similar richness values to those found in the optimized community of the long-term experiment. The average richness values of the optimized community were 196.9 ± 16.7 and 62.4 ± 12.4 for the bacterial and archaeal communities, respectively. Similarly, the average richness values of the start-up communities for the single B-shock were 199.4 ± 9.3 and 62.0 ±5.7, and for the single C-shock were 201.8± 9.9 and 62.2 ± 6.8, for the bacterial and archaeal communities, respectively.

However, unlike during the long-term experiment, the single-shock microbiomes were not exposed to small organic loads (A-shocks) prior to the single moderate B- and single large C-shock events. As such, when exposed to a single B-shock, instead of observing enhanced performance, or the shifting of the microbiome to a more optimal configuration, reactor performance showed signs of failure and the microbiome had low diversity metrics and a high level of dissimilarity compared to the optimized microbiome observed during the long-term experiment (0.789 for Bacteria and 1.000 for Archaea).

Similarly, when exposed to a single C-shock, failure again ensued as did a high level of dissimilarity compared to the optimized microbiome observed during the long-term experiment (0.877 for Bacteria and 1.000 for Archaea). Additionally, the recovery time was greater than that observed in the long-term experiments for a similar level of failure. Thus, the enrichment of certain microbes (primarily from the A- shocks) is a critical step in enhancing anaerobic digester performance and robustness for FOG co-digestion.

Thus, all four community diversity metrics (richness, evenness, PCoA, and Raup and Crick dissimilarity) demonstrated that although each exposure to FOG had some effect on the microbiome structure, noteworthy changes were only observed once failure was observed. In general, the bacterial domain exhibited greater changes than the archaeal domain, likely due to the increased functional redundancy and diversity within the bacterial domain (Wang et al., 2020). When these disturbance-to-failure events occur, the microbiome structure does not return to its original state but takes on a new and unique structure (Fig. 2). Additionally, diversity itself is not sufficient for prediction of reactor performance or resilience.

3.3. Response of the dominant bacterial community to FOG shock loads

The taxonomic distribution of the bacterial ASVs showed that the majority of the ASVs present were classified as sub-dominant with median relative abundance values of < 1.5% (Fig. 4). The 1.5% sub-dominant threshold was chosen to improve visualization of taxonomic profiles. Only 11 bacterial genera had a median relative abundance>1.5% (dominant bacteria), but collectively accounted for 18–93% of the total sequences present.

Following non-failure-inducing events (e.g. B1-B3 shocks), these dominant taxa make up a smaller fraction of the sequences per sample than they do during post-failure recovery periods. Following the moderate, non-failure inducing B1-B3 shocks, these dominant taxa only make up 23–41% of the community. However, following the large, failure-inducing C1-C3 shocks) these dominant taxa account for 68–93% in the early recovery phase and 22–61% in the later recovery phase. This suggests that the sub-dominant taxa are largely responsible for normal digester operation and the dominant taxa are necessary and specific to reactor recovery. Sub-dominant taxa (as low as 0.1%) have been previously suggested to play important roles in maintaining anaerobic digester stability and functionality (Guo et al., 2022).

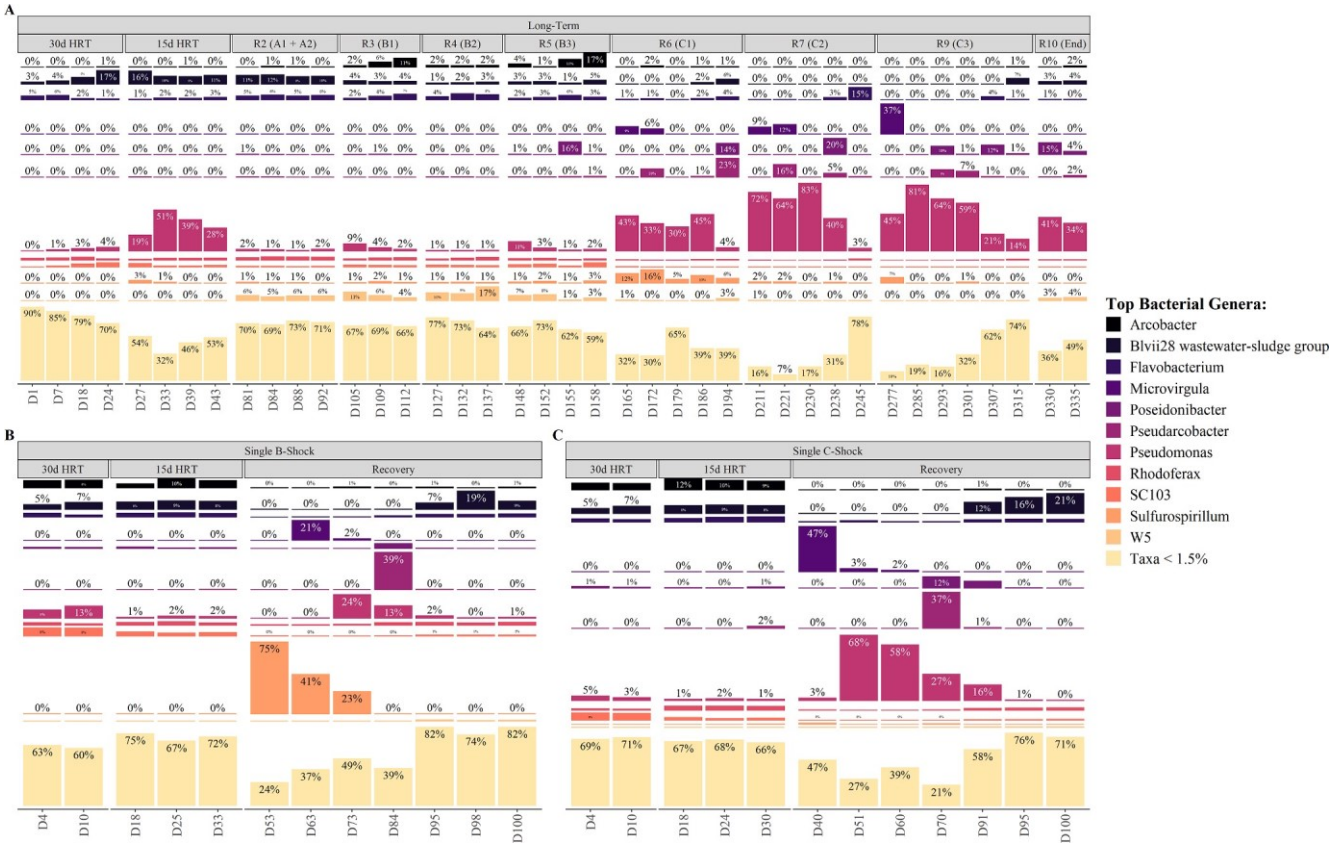

Fig. 4. Relative abundances of bacterial genera during all three experiments. Sub-dominant ASVs, those with a median relative abundance of <1.5%, are grouped into one bar.

The most abundant bacterial genera during the start-up of all 3 experiments were *Arcobacter*, *Blvii28 wastewater sludge group*, and *Pseudomonas* (Fig. 4). During the long-term experiment, the bacterial genera *Flavobacterium*, *Rhodoferax*, and *W5* were enriched after the two small A shock loads. As the successive moderate B shock loads were employed, *Blvii28 wastewater-sludge group* decreased while *W5* increased. Finally, following the disturbance-to-failure events experienced in all experiments, the most abundant bacterial genera initially were *Pseudomonas* and *Micorvirgula*, which both decreased in abundance at the end of each respective recovery period, and were later replaced by sub-dominant taxa. *Sulfurospirillum* and *Pseudoarcobacter* were also dominant following the single-shock disturbance-to-failure events (Fig. 4).

Of the dominant taxa, the following five are considered to be common wastewater sludge bacteria observed in anaerobic digestion systems: *Arcobacter*, *Blvii28 wastewater-sludge group*, *Poseidonibacter*, *Pseudoarcobacter*, and *SC103* (Kristensen et al., 2020; Nierychlo et al., 2020; Su et al., 2014). Two of these five, *Poseidonibacter* and *Pseudoarcobacter* were not significantly correlated with any of the operational parameters investigated. The other 3 correlated with parameters indicative of normal digester operation, such as elevated pH values, elevated methane content, and low OA, TS, and VS values (Fig. 5).

Flavobacterium and *Rhodoferax* were significantly correlated with normal AD performance, while *W5* were significantly correlated with parameters indicative of enhanced AD performance. Specifically, *Flavobacterium* and *Rhodoferax* were correlated with elevated pH and methane content values and decreased solids and OA values, while *W5* was significantly correlated with elevated OLR, biogas, and methane content values. *Flavobacterium* spp. are typically associated with the degradation of proteins and carbohydrates while *W5* spp. aid with later stages of fermentation and are likely propionate oxidizers (Dyksma and Gallert, 2019; Sposob et al., 2021). *Flavobacterium* spp. have also been identified as some of the most common taxa in anaerobic digesters fed municipal sludge and have been observed at elevated levels in co-digestion systems receiving food waste (Sposob et al., 2021; Sundberg et al., 2013). *Rhodoferax* spp. are metabolically complex facultative anaerobes that are predominant in activated sludge but also appear in anaerobic digesters with short sludge retention times (Tonanzi et al., 2021).

Pseudomonas, *Sulfurospirillum*, and *Microvirgula* were significantly correlated with parameters indicative of reactor failure (i.e. decreased biogas production, methane content, and increased OA, TS and VS values). *Pseudomonas* spp. are key players for all methanogenic pathways and are mainly active during hydrolysis of carbohydrates, although they have been shown utilize LCFAs (Buettner et al., 2019; Fontaine et al., 2017). *Pseudomonas*' key contribution to hydrolysis explains their ubiquitous presence and increased abundance during the start of reactor failure when OA accumulation was at its greatest. As such, this genus has been previously observed to be prevalent across a wide variety of AD systems (De Vrieze et al., 2015). Conversely, the presence of *Microvirgula* and *Sulfurospirillum* were likely due to the increased ratio of RAS fed during recovery periods, as they have been observed previously in wastewater systems (Kruse et al., 2018; S´wiątczak and Cydzik-Kwiatkowska, 2018).

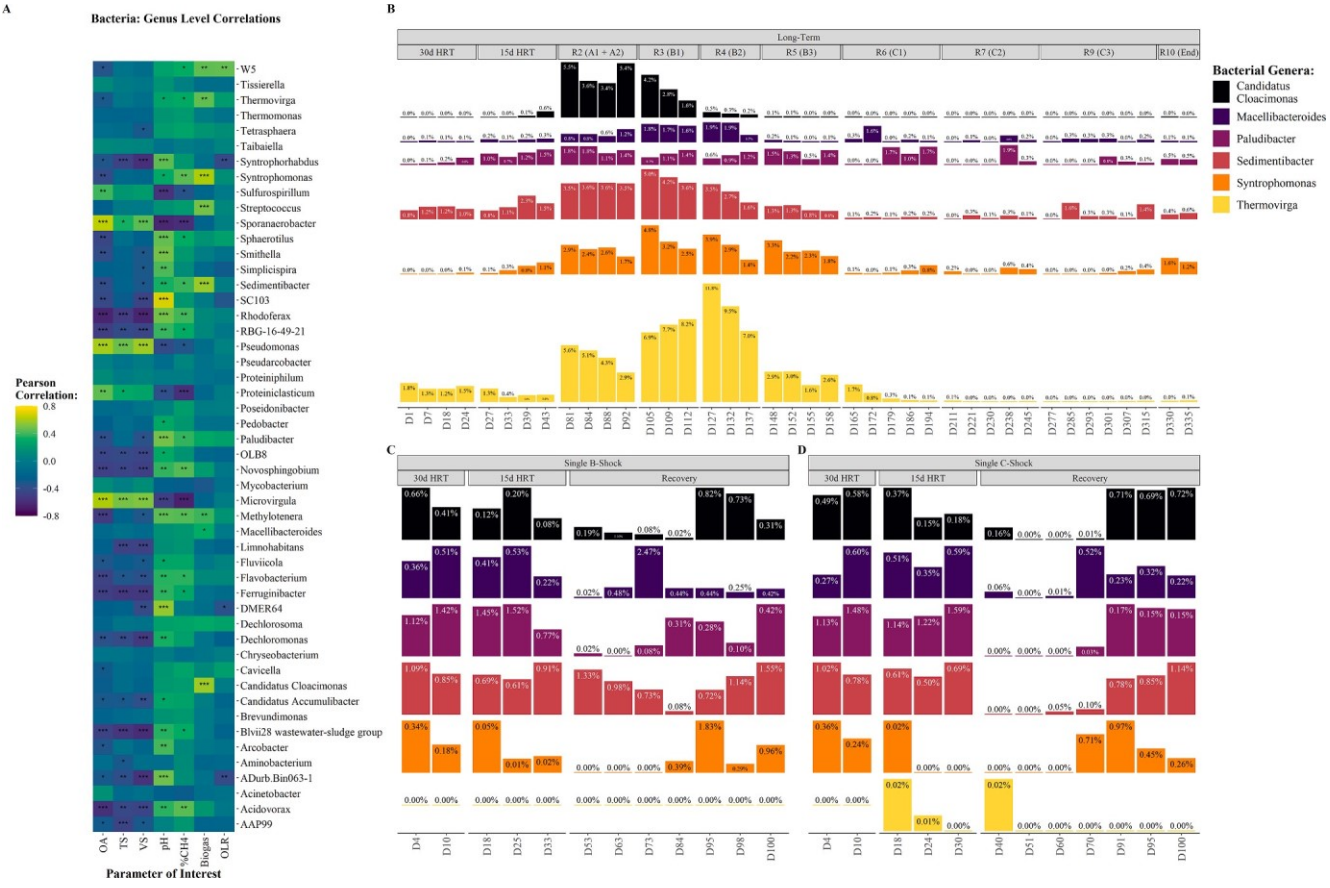

Fig. 5. Pearson correlations between the top 50 bacterial genera and chosen operational parameters of interest (A). Operational parameters of interest are as follows: OA (organic acids), TS (total solids), VS (volatile solids), pH, % CH_4, Biogas, and OLR (organic loading rate). Shading was done based on the Pearson correlation values. Stars (*) within specific cells indicate significance of that correlation: * 90%, ** 95%, and *** 99%. Relative abundance values for bacterial genera of interest for the long-term (B) and single-shock (C-D) experiments.

3.4. Response of the sub-dominant bacterial community to FOG shock loads

In all experiments, sub-dominant bacterial taxa (<1.5% median relative abundance) accounted for 7−90% of the ASVs present. After non-failure-inducing shock events, the percentage of sub-dominant bacteria remained above 60% (Fig. 4). However, after failure-inducing shock events, the sub-dominant taxa represented as little as 7% of the ASVs present before rising again at the end of the recovery period. These shifts in sub-dominant relative abundance values mirrored what was observed with the richness and Shannon alpha diversity metrics (Fig. 2).

Of the top 50 bacterial genera, 17 demonstrated a statistically significant (>90% confidence) positive correlation with biogas production and/or methane content (Fig. 5). Of these 17 bacterial genera, 13 were classified as sub-dominant (<1.5% median relative abundance). Additionally, there were 5 separate bacterial genera that showed a significant positive correlation with indicators of reactor failure (i.e. decreased biogas production, methane content, and increased OA, TS, and VS values). Of these 5 bacterial genera, 2 were classified as sub-dominant. *Thermovirga*, *Syntrophomonas*, *Sedimentibacter*, and *Candidatus Cloacimonas* showed significant positive correlations with biogas production and/or methane content. All 4 bacterial genera have been previously reported to have been enriched under increased FOG loads (Wang et al., 2020). In the long-term study, *Thermovirga* was initially enriched after the two small A-shock loads and continued to increase in abundance through the successive moderate B-shock loads, but was relatively unobserved in the single-shock studies (Fig. 5).

Thermovirga and *Sedimentibacter* both contribute to hydrolytic processes (Sposob et al., 2021), while *Syntrophomonas* is comprised mostly of syntrophic acetate oxidizers capable of metabolizing LCFAs (Ziels et al., 2017). Additionally, all four of these bacterial genera, sans *Candidatus Cloacimonas*, a likely syntrophic propionate oxidizing bacteria, significantly correlated negatively with OA accumulation (Dyksma and Gallert, 2019) (Fig. 5). Thus, their enrichment suggests the successful adaptation of the reactor to FOG co-digestion in which hydrolysis reactions are in balance with OA accumulation (Wang et al., 2020).

Paludibacter and *Macellibacteroides*, both fermenters, were also positively correlated with biogas production and/or methane content. *Paludibacter* ferments carbohydrates and proteins into primarily acetate and propionate (Sposob et al., 2021). *Macellibacteroides* is a sugar fermenter and produces primarily lactate, acetate, butyrate and isobutyrate (Jabari et al., 2012). Both *Paludibacter* and *Macellibacteroides* are commonly found in both mono- and co-substrate anaerobic digesters (Mercado et al., 2022; Sposob et al., 2021).

Finally, 6 other sub-dominant genera correlated with increased biogas and/or methane production. These included the following; *Streptococcus*, a common wastewater pathogen (Finley et al., 2009), *Methylotenera*, a ubiquitous obligate methylotroph (Beck et al., 2011), *Sphaerotilus*, a filamentous aerobic bacteria associated with bulking sludge, *RBG-16−49-21* and *Acidovorax*, both considered denitrifying activated sludge bacteria, and *Novosphingobium* and *Ferruginibacter*, both aerobic heterotrophs commonly observed in wastewater (Nierychlo et al., 2020; Sposob et al., 2021). As all of these sub-dominant genera are common in wastewater treatment systems, it is likely that the strong correlations observed are due to the increased ratio of TWAS in the influent during the phases that exhibited greater biogas productivity and not a sign of their active contribution to the anaerobic digestion process.

Both *Sporanaerobacter* and *Proteiniclasticum* were enriched during times of reactor upset and contributed to the early recovery stages as indicated by their correlations with decreased pH and methane content along with increased OA and total solids concentrations. *Sporanaerobacter* and *Proteiniclasticum* are both acetogenic genera capable of producing several OAs, including acetate, isobutyrate, isovalerate, and propionate through the fermentation of the proteinaceous fractions of complex wastes as observed in other AD studies (Kurade et al., 2019; Ziganshina et al., 2014). Although these two genera are considered sub-dominant (<1.5% median relative abundance), the degradation of proteinaceous components of FOG is an essential fermentation step and their presence in the early stages of failure is clearly indicated based on their strong correlations with operational indicators of failure.

3.5. Response of the archaeal community to FOG shock loads

Within the archaeal domain only 8 genera had a median relative abundance >1.5%, but collectively accounted for 77−99% of the total ASVs present. The most abundant archaeal genera were *Methanolinea*, a hydrogenotrophic methanogen, and *Methanosaeta*, an acetoclastic methanogen (Leng et al., 2018). Due to the small number of methanogenic genera, the sub-dominant archaeal taxa did not fluctuate as greatly as did the sub-dominant bacterial taxa after disturbance-to-failure events. This resulted in fewer statistically significant correlations with process performance. However, there are still distinct early and late post-failure recovery trends, especially between *Methanosaeta* (acetoclastic pathway) during early recovery and *Methanosarcina* (mixed pathway) in late recovery (Leng et al., 2018).

Archaeal relative abundance data was aggregated based on methanogenic metabolism to highlight functional shifts over time. During start-up in all three experiments, the methanogenic community was primarily dominated by acetoclastic *Methanosaeta* and hydrogenotrophic *Methanolinea* (Fig. 6 B-D). The order of the relative abundance ranking of *Methanosaeta* and *Methanolinea* varied between experiments, but they were always the top two genera present. The aggregated hydrogenotrophic and acetoclastic communities comprised 34−57% and 32−60%, respectively, of the methanogens initially present. The methylotrophic community, mainly *Methanomassiliicoccus*, represented 4−14% of the archaeal ASVs present (Cozannet et al., 2020).

The optimized community created via the small (A1-A2) and moderate (B1-B3) shocks employed during the long-term experiment saw an overall decrease and diversification of the hydrogenotrophic community. Specifically, the abundance of *Methanolinea* decreased while the abundances of the sub-dominant *Methanobacterium* and the dominant *Methanoculleus* increased (Leng et al., 2018; Liu and Whitman, 2008). *Methanobacterium* and *Methanoculleus* each had significant positive correlations with biogas production and methane composition, respectively, indicating their importance for improved methane production (Fig. 6).

In addition to the decrease in the hydrogenotrophic pathway, the optimized community also saw an enrichment of methylotrophic *Methanomassiliicoccus*. *Methanomassiliicoccus* had significant positive correlations with biogas production and methane composition, indicating the importance utilizing methylated compounds via the methylotrophic pathway in enhancing biogas and methane production. Finally, acetoclastic *Methanosaeta* remained relatively stable from the start-up to the optimized community (Fig. 6).

Immediately following the failure-inducing shocks in both the single-shock and long-term experiments, the total methanogen population decreased, as measured via quantification of the *mcrA* gene (Berninghaus and Radniecki, 2022). Of the remaining methanogens, acetoclastic *Methanosaeta* was enriched and dominated the methanogenic community while the methylotrophic aggregate decreased due to decreases in the relative abundances of both *Methanomassiliicoccus* and sub-dominant *Methanomethylovorans* (Leng et al., 2018).

Additionally, immediately after failure, the hydrogenotrophic pathway also decreased due to decreases in the relative abundance of *Methanolinea*, *Methanobacterium*, and *Methanoculleus* (Fig. 6). However, two hydrogenotrophic methanogens, *Methanospirillum* (during the long-term experiments) and *Methanobrevibacter* (during the single shock experiments), were enriched and became the dominant methylotrophic organisms during this period (Leng et al., 2018). Both had significant positive correlations with OA and negative correlations with pH, indicating their importance during times of organic overloads. *Methanospirillum* has been previously shown to potentially prefer a high-fat

Fig 6. Pearson correlations between the top 50 archaeal genera and chosen operational parameters of interest (A). Operational parameters of interest are as follows: OA (organic acids), TS (total solids), VS (volatile solids), pH, % CH_4, Biogas, and OLR (organic loading rate). Shading was done based on the Pearson correlation values. Stars (*) within specific cells indicate significance of that correlation: * 90%, ** 95%, and *** 99%. Relative abundance values for bacterial genera of interest for the long-term (B) and single shock (C-D) experiments. Sub-dominant ASVs, with a median relative abundance of <1.5%, are grouped into one bar.

environment further explaining its presence early in the recovery phases (Wang et al., 2020).

During the recovery from failure, in all three experiments, the acetoclastic methanogen *Methanosaeta* performed a bimodal recovery with *Methanosarcina* (mixed pathways), as has been observed previously (Kurade et al., 2019). Early in recovery, acetoclastic methanogenesis via *Methanosaeta* occurred as OAs built up in response to the organic overload event while *Methanosarcina* became dominant later in the recovery as the OAs began to deplete (Figs. 1 and 6) (Berninghaus and Radniecki, 2022). It is assumed that *Methanosarcina* was contributing to acetoclastic methanogenesis due to the amount of OA accumulation that remained, however, due to the metabolic diversity of *Methanosarcina*, this cannot be stated with certainty.

The initial dominance of *Methanosaeta* during start-up and non-failure-inducing shocks was likely due to the low acetate concentrations (<1 g/L) present in the digesters (Figs. 1 and 6). Under these conditions, *Methanosaeta* was able to outcompete *Methanosarcina* due to its higher substrate affinity (with an order of magnitude smaller half saturation constant - K_s) (Conklin et al., 2006; De Vrieze et al., 2012). *Methanosaeta* continued to dominate initially after the failure-inducing shocks due to its higher tolerance to LCFAs (Conklin et al., 2006; Silva et al., 2016). The hydrolysis of FOG and the accompanying LCFAs is a rate-limiting step during FOG co-digestion and likely lingered in the digesters immediately following a failure-inducing shock (Angelidaki and Ahring, 1992; Ziels et al., 2016).

However, as the LCFAs were hydrolyzed, the levels of acetate in the digesters remained elevated for an extended period (>1 g/L for > 14 days) (Fig. 1). This allowed for *Methanosarcina* to become dominant, taking advantage of its 3-fold higher maximum specific growth rate (μ_{max}) (Conklin et al., 2006; De Vrieze et al., 2012). As the acetate levels decreased during each recovery period, so did the relative abundance of *Methanosarcina* (Figs. 1 and 6). Nonetheless, at the end of each experiment, *Methanosarcina* retained a relative abundance greater than its pre-failure values while *Methanosaeta* sustained below pre-failure abundances.

Recovery from both single-shock events resulted in the enrichment of both the hydrogenotrophic and methylotrophic methanogenic pathways. *Methanofollis* (hydrogenotrophic) (Liu and Whitman, 2008), became dominant in the single moderate B-shock experiment, while the large single C-shock experiment exhibited a more even distribution of the top hydrogenotrophic genera.

Additionally, the metabolically diverse *Methanosarcina* became dominant during middle of the recovery before yielding to the methylotrophic *Candidatus Methanofastidiosum* and *Methanomassiliicoccus* by the end of both single-shock experiments (Fig. 6C and D). *Candidatus Methanofastidiosum* strongly correlated with four of the seven parameters of interest including a negative correlation with OAs and solids content as well as a positive correlation with pH, indicating its importance during late stage recovery (Vanwonterghem et al., 2016) (Fig. 6A). A similar pattern was observed during the first failure event (C1) of the long-term experiment with an initial enrichment of the acetoclastic pathway and decreases in the hydrogenotrophic and methylotrophic pathways. However, unlike in the single-shock experiments, the methylotrophic pathway did not recover to its pre-failure relative abundance level by the end of the recovery period. Instead, *Methanosarcina* maintained a sizable relative abundance. Thus, the recovered archaeal community did not mirror the optimized community but instead, created a new one.

When exposed to additional failure inducing shock loads (C2 and C3), this new archaeal community was not as robust as the optimized community that experienced the initial failure-inducing shock-load (C1). The new archaeal communities took longer to degrade OAs and regain biogas production rates (Fig. 1). Additionally, the microbiome responses were different. *Methanosaeta* was still initially enriched and then decreased corresponding with the emergence of *Methanosarcina*. However, with each successive C-shock, *Methanosarcina* was enriched earlier in the recovery and to higher levels of relative abundance. This resulted in the near complete elimination of the methylotrophic pathway while the hydrogenotrophic pathway did maintain a fairly stable relative abundance (Fig. 6B).

The increasing dominance of *Methosarcina* and decrease of other methanogens with each successive failure-inducing shock load may help to explain the increasing time to recovery. Although *Methanosarcina* is capable of exploiting the three main methanogenic pathways, it can be assumed that each pathway would be utilized in order of free energy released, one after another. This is in contrast with a more metabolically diverse methanogen community where all three pathways could be utilized simultaneously by different groups of methanogens.

4. Conclusions

Repeated small and moderate shocks enriched the fermenters *Flavobacterium*, *Thermovirga*, *W5* as well as *Methanosaeta*, *Methanomassiliicoccus*, and *Methanomethyliaceae*, with sub-dominant bacterial largely responsible for increased biogas production. Failure-inducing shocks created a clear delineation between early and late recovery microbiomes. Initially, acetoclastic *Methanosaeta* were dominant but were replaced by *Methanosarcina*. Similarly, *Pseudomonas* were dominant in early recovery while sub-dominant bacterial taxa were enriched in late recovery. Post-failure microbiomes were divergent from both the initial and FOG-optimized microbiomes. Thus, while non-failure inducing loads can optimize microbiomes for FOG co-digestion, failure events undo this optimization and adaptation processes must begin again.

CRediT authorship contribution statement

Ashley E. Berninghaus: Conceptualization, Methodology, Experimentation, Data Collection, Interpretation, Data Visualization, Writing − original manuscript and editing. **Tyler S. Radniecki:** Conceptualization, Interpretation, Supervision, Funding Acquisition, Writing − reviewing and editing.

Declaration of Competing Interest

The authors declare that they have no known competing financial interests or personal relationships that could have appeared to influence the work reported in this paper.

Acknowledgments

This study was supported by the NSF CAREER Grant #1847654. The authors thank the individuals who aided in sequencing efforts at the Center for Quantitative Life Sciences, especially Mark Dasenko. The authors are particularly grateful to the staff of the City of Corvallis Wastewater Reclamation Plant for their assistance with sample collection and to the staff at Jacobs Engineering Inc. who run the City of Gresham Wastewater Reclamation Plant for their assistance with FOG collection.

Appendix A. Supplementary data

Supplementary data to this article can be found online at https://doi.org/10.1016/j.biortech.2022.127400.

References

Amha, Y.M., Sinha, P., Lagman, J., Gregori, M., Smith, A.L., 2017. Elucidating microbial community adaptation to anaerobic co-digestion of fats, oils, and grease and food waste. Water Res. 123, 277–289.

Angelidaki, I., Ahring, B., 1992. Ahring, B.: Effects of free long-chain fatty acids on thermophilic anaerobic digestion. Appl. Microbiol. Biotechnol. 37 (6), 808–812.

Apprill, A., McNally, S., Parsons, R., Weber, L., 2015. Minor revision to V4 region SSU rRNA 806R gene primer greatly increases detection of SAR11 bacterioplankton. Aquat. Microb. Ecol. 75 (2), 129–137.

Beck, D.A.C., Hendrickson, E.L., Vorobev, A., Wang, T., Lim, S., Kalyuzhnaya, M.G., Lidstrom, M.E., Hackett, M., Chistoserdova, L., 2011. An integrated proteomics/transcriptomics approach points to oxygen as the main electron sink for methanol metabolism in Methylotenera mobilis. J. Bacteriol. 193 (18), 4758–4765.

Berninghaus, A.E., Radniecki, T.S. 2021. Fats, Oils, and Greases Increase the Sensitivity of Anaerobic Mono- and Co-Digester Inoculum to Ammonia Toxicity. *Environmental Engineering Science*, **Online ahead of print**.

Berninghaus, A.E., Radniecki, T.S., 2022. Shock loads change the resistance, resiliency, and productivity of anaerobic co-digestion of municipal sludge and fats, oils. and Greases. Under Review.

Buettner, C., von Bergen, M., Jehmlich, N., Noll, M., 2019. Pseudomonas spp. are key players in agricultural biogas substrate degradation. Sci. Rep. 9 (1), 12871.

Chase, J.M., Kraft, N.J.B., Smith, K.G., Vellend, M., Inouye, B.D., 2011. Using null models to disentangle variation in community dissimilarity from variation in α-diversity. Ecosphere 2 (2), art24.

Conklin, A., Stensel, H.D., Ferguson, J., 2006. Growth kinetics and competition between Methanosarcina and Methanosaeta in mesophilic anaerobic digestion. Water Environ Res 78 (5), 486–496.

Cozannet, M., Borrel, G., Roussel, E., Moalic, Y., Allioux, M., Sanvoisin, A., Toffin, L., Alain, K., 2020. New Insights into the Ecology and Physiology of Methanomassiliicoccales from Terrestrial and Aquatic Environments. Microorganisms 9 (1), 30.

De Vrieze, J., Hennebel, T., Boon, N., Verstraete, W., 2012. Methanosarcina: the rediscovered methanogen for heavy duty biomethanation. Bioresour Technol 112, 1–9.

De Vrieze, J., Saunders, A.M., He, Y., Fang, J., Nielsen, P.H., Verstraete, W., Boon, N., 2015. Ammonia and temperature determine potential clustering in the anaerobic digestion microbiome. Water Res. 75, 312–323.

Dyksma, S., Gallert, C., 2019. Candidatus Syntrophosphaera thermopropionivorans: a novel player in syntrophic propionate oxidation during anaerobic digestion. Environmental Microbiology Reports 11 (4), 558–570.

Ferguson, R.M.W., Coulon, F., Villa, R., 2018. Understanding microbial ecology can help improve biogas production in AD. Sci Total Environ 642, 754–763.

Finley, S., Barrington, S., Lyew, D., 2009. Reuse of Domestic Greywater for the Irrigation of Food Crops. Water Air Soil Pollut. 199 (1), 235–245.

Fischer, M.A., Gullert, S., Refai, S., Kunzel, S., Deppenmeier, U., Streit, W.R., Schmitz, R. A., 2019. Long-term investigation of microbial community composition and transcription patterns in a biogas plant undergoing ammonia crisis. Microb Biotechnol 12 (2), 305–323.

Fontaine, P., Mosrati, R., Corroler, D., 2017. Medium chain length polyhydroxyalkanoates biosynthesis in Pseudomonas putida mt-2 is enhanced by co-metabolism of glycerol/octanoate or fatty acids mixtures. Int J Biol Macromol 98, 430–435.

Guo, B., Zhang, L., Sun, H., Gao, M., Yu, N., Zhang, Q., Mou, A., Liu, Y., 2022. Microbial co-occurrence network topological properties link with reactor parameters and reveal importance of low-abundance genera. npj Biofilms Microbiomes 8 (1), 3.

Jabari, L., Gannoun, H., Cayol, J.-L., Hedi, A., Sakamoto, M., Falsen, E., Ohkuma, M., Hamdi, M., Fauque, G., Ollivier, B., Fardeau, M.-L., 2012. Macellibacteroides fermentans gen. nov., sp. nov., a member of the family Porphyromonadaceae isolated from an upflow anaerobic filter treating abattoir wastewaters. Int. J. Syst. Evol. Microbiol. 62 (Pt_10), 2522–2527.

Jari Oksanen, F.G.B., Michael Friendly, Roeland Kindt, Pierre Legendre, Dan McGlinn, Peter R. Minchin, R. B. O'Hara, Gavin L. Simpson, Peter Solymos, M. Henry H. Stevens, Eduard Szoecs and Helene Wagner 20vegan: Community Ecology Package. R package version 2.5-7 ed.

Knight, R., Vrbanac, A., Taylor, B.C., Aksenov, A., Callewaert, C., Debelius, J., Gonzalez, A., Kosciolek, T., McCall, L.-I., McDonald, D., Melnik, A.V., Morton, J.T., Navas, J., Quinn, R.A., Sanders, J.G., Swafford, A.D., Thompson, L.R., Tripathi, A., Xu, Z.Z., Zaneveld, J.R., Zhu, Q., Caporaso, J.G., Dorrestein, P.C., 2018. Best practices for analysing microbiomes. Nat. Rev. Microbiol. 16 (7), 410–422.

Kougias, P.G., Treu, L., Campanaro, S., Zhu, X., Angelidaki, I., 2016. Dynamic functional characterization and phylogenetic changes due to Long Chain Fatty Acids pulses in biogas reactors. Sci. Rep. 6 (1), 28810.

Kristensen, J.M., Nierychlo, M., Albertsen, M., Nielsen, P.H., Zhou, N.-Y. 2020. Bacteria from the Genus Arcobacter Are Abundant in Effluent from Wastewater Treatment Plants. *Applied and Environmental Microbiology*, **86**(9), e03044-19.

Kruse, S., Goris, T., Westermann, M., Adrian, L., Diekert, G., 2018. Hydrogen production by Sulfurospirillum species enables syntrophic interactions of Epsilonproteobacteria. Nat. Commun. 9 (1), 4872.

Kurade, M.B., Saha, S., Salama, E.-S., Patil, S.M., Govindwar, S.P., Jeon, B.-H., 2019. Acetoclastic methanogenesis led by Methanosarcina in anaerobic co-digestion of fats, oil and grease for enhanced production of methane. Bioresour. Technol. 272, 351–359.

Leng, L., Yang, P., Singh, S., Zhuang, H., Xu, L., Chen, W.-H., Dolfing, J., Li, D., Zhang, Y., Zeng, H., Chu, W., Lee, P.-H., 2018. A review on the bioenergetics of anaerobic

microbial metabolism close to the thermodynamic limits and its implications for digestion applications. Bioresour. Technol. 247, 1095–1106.
Li, C., Champagne, P., Anderson, B.C., 2013. Biogas production performance of mesophilic and thermophilic anaerobic co-digestion with fat, oil, and grease in semi-continuous flow digesters: effects of temperature, hydraulic retention time, and organic loading rate. Environ. Technol. 34 (13–14), 2125–2133.
Liu, C., Cui, Y., Li, X., Yao, M., 2020. microeco: an R package for data mining in microbial community ecology. FEMS Microbiol. Ecol. 97 (2).
Liu, Y., Whitman, W.B., 2008. Metabolic, Phylogenetic, and Ecological Diversity of the Methanogenic Archaea. Ann. N. Y. Acad. Sci. 1125 (1), 171–189.
McMurdie, P.J., Holmes, S., 2013. phyloseq: An R Package for Reproducible Interactive Analysis and Graphics of Microbiome Census Data. PLoS ONE 8 (4), e61217.
Mercado, J.V., Koyama, M., Nakasaki, K., 2022. Short-term changes in the anaerobic digestion microbiome and biochemical pathways with changes in organic load. Sci. Total Environ. 813, 152585.
Nierychlo, M., Andersen, K.S., Xu, Y., Green, N., Jiang, C., Albertsen, M., Dueholm, M.S., Nielsen, P.H., 2020. MiDAS 3: An ecosystem-specific reference database, taxonomy and knowledge platform for activated sludge and anaerobic digesters reveals species-level microbiome composition of activated sludge. Water Res. 182, 115955.
Parada, A.E., Needham, D.M., Fuhrman, J.A., 2016. Every base matters: assessing small subunit rRNA primers for marine microbiomes with mock communities, time series and global field samples. Environ. Microbiol. 18 (5), 1403–1414.
Salama, E.-S., Saha, S., Kurade, M.B., Dev, S., Chang, S.W., Jeon, B.-H., 2019. Recent trends in anaerobic co-digestion: Fat, oil, and grease (FOG) for enhanced biomethanation. Prog. Energy Combust. Sci. 70, 22–42.
Silva, S.A., Salvador, A.F., Cavaleiro, A.J., Pereira, M.A., Stams, A.J., Alves, M.M., Sousa, D.Z., 2016. Toxicity of long chain fatty acids towards acetate conversion by Methanosaeta concilii and Methanosarcina mazei. Microb Biotechnol 9 (4), 514–518.
Silvestre, G., Rodríguez-Abalde, A., Fern´andez, B., Flotats, X., Bonmatí, A., 2011. Biomass adaptation over anaerobic co-digestion of sewage sludge and trapped grease waste. Bioresour. Technol. 102 (13), 6830–6836.
Sposob, M., Moon, H.-S., Lee, D., Yun, Y.-M., 2021. Microbiome of Seven Full-Scale Anaerobic Digestion Plants in South Korea: Effect of Feedstock and Operational Parameters. Energies 14 (3), 665.
Su, X.-L., Tian, Q., Zhang, J., Yuan, X.-Z., Shi, X.-S., Guo, R.-B., Qiu, Y.-L., 2014. Acetobacteroides hydrogenigenes gen. nov., sp. nov., an anaerobic hydrogen-producing bacterium in the family Rikenellaceae isolated from a reed swamp. Int. J. Syst. Evol. Microbiol. 64 (Pt_9), 2986–2991.
Sundberg, C., Al-Soud, W.A., Larsson, M., Alm, E., Yekta, S.S., Svensson, B.H., Sørensen, S.J., Karlsson, A., 2013. 454 pyrosequencing analyses of bacterial and archaeal richness in 21 full-scale biogas digesters. FEMS Microbiol. Ecol. 85 (3), 612–626.
S´wiątczak, P., Cydzik-Kwiatkowska, A., 2018. Treatment of Ammonium-Rich Digestate from Methane Fermentation Using Aerobic Granular Sludge. Water Air Soil Pollut. 229 (8), 247.
Tonanzi, B., Crognale, S., Gianico, A., Della Sala, S., Miana, P., Zaccone, M.C., Rossetti, S., 2021. Microbial Community Successional Changes in a Full-Scale Mesophilic Anaerobic Digester from the Start-Up to the Steady-State Conditions. Microorganisms 9 (12), 2581.
Vanwonterghem, I., Evans, P.N., Parks, D.H., Jensen, P.D., Woodcroft, B.J., Hugenholtz, P., Tyson, G.W., 2016. Methylotrophic methanogenesis discovered in the archaeal phylum Verstraetearchaeota. Nat. Microbiol. 1 (12), 16170.
Wang, L., Hossen, E.H., Aziz, T.N., Ducoste, J.J., de los Reyes, F.L., 2020. Increased loading stress leads to convergence of microbial communities and high methane yields in adapted anaerobic co-digesters. Water Res. 169, 115155.
Wang, P., Wang, H., Qiu, Y., Ren, L., Jiang, B., 2018. Microbial characteristics in anaerobic digestion process of food waste for methane production–A review. Bioresour. Technol. 248, 29–36.
Werner, J.J., Garcia, M.L., Perkins, S.D., Yarasheski, K.E., Smith, S.R., Muegge, B.D., Stadermann, F.J., DeRito, C.M., Floss, C., Madsen, E.L., Gordon, J.I., Angenent, L.T., Spormann, A.M., 2014. Microbial Community Dynamics and Stability during an Ammonia-Induced Shift to Syntrophic Acetate Oxidation. Appl. Environ. Microbiol. 80 (11), 3375–3383.
Yang, Z.H., Xu, R., Zheng, Y., Chen, T., Zhao, L.J., Li, M., 2016. Characterization of extracellular polymeric substances and microbial diversity in anaerobic co-digestion reactor treated sewage sludge with fat, oil, grease. Bioresour Technol 212, 164–173.
Yu, Y., Lee, C., Kim, J., Hwang, S., 2005. Group-specific primer and probe sets to detect methanogenic communities using quantitative real-time polymerase chain reaction. Biotechnol Bioeng 89 (6), 670–679.
Ziels, R.M., Beck, D.A.C., Stensel, H.D., 2017. Long-chain fatty acid feeding frequency in anaerobic codigestion impacts syntrophic community structure and biokinetics. Water Res. 117, 218–229.
Ziels, R.M., Karlsson, A., Beck, D.A.C., Ejlertsson, J., Yekta, S.S., Bjorn, A., Stensel, H.D., Svensson, B.H., 2016. Microbial community adaptation influences long-chain fatty acid conversion during anaerobic codigestion of fats, oils, and grease with municipal sludge. Water Res. 103, 372–382.
Ziganshina, E.E., Belostotskiy, D.E., Shushlyaev, R.V., Miluykov, V.A., Vankov, P.Y., Ziganshin, A.M., 2014. Microbial community diversity in anaerobic reactors digesting turkey, chicken, and swine wastes. J Microbiol Biotechnol 24 (11), 1464–1772.